Innovative Food Science and Emerging Technologies 56 (2019) 102182

Contents lists available at ScienceDirect

Innovative Food Science and Emerging Technologies

journal homepage: www.elsevier.com/locate/ifset

Combined radio frequency-vacuum and hot air drying of kiwifruits: Effect on drying uniformity, energy efficiency and product quality

Xu Zhou[a], Hosahalli Ramaswamy[b], Yingtao Qu[a], Ruzhen Xu[a], Shaojin Wang[a,c,*]

[a] College of Mechanical and Electronic Engineering, Northwest A&F University, Yangling, Shaanxi 712100, China
[b] Department of Food Science and Agricultural Chemistry, McGill University, Montreal H9X 3V9, Canada
[c] Department of Biological Systems Engineering, Washington State University, 213 L.J. Smith Hall, Pullman, WA 99164-6120, USA

ARTICLE INFO

Keywords:
Radio frequency-vacuum drying
Hot air drying
Heating uniformity index
Moisture distribution
Kiwifruit

ABSTRACT

Two drying methods, both individually and in their combination [RF-vacuum drying (RFVD), hot air drying (HAD) and RFVD + HAD] were evaluated for three-layer drying of 6 mm thick kiwifruit slices in order to shorten drying time, improve energy efficiency and product quality. An electrode gap of 95 mm and vacuum of 20.1 kPa were selected for RFVD applications based on previous studies. Results showed that the total drying time was the shortest (480 min) when using RFVD, followed by RFVD + HAD (600 min; 20% longer) and HAD (900 min, almost double). However, non-uniform drying patterns were observed in both RFVD and HAD methods, but the RFVD + HAD process resulted in a more uniform moisture distribution both within and among the fruit slices. The average energy efficiency of HAD was improved remarkably from 9.92% to 22.93% by applying the RFVD + HAD method. Additionally, the RFVD + HAD process resulted in better product quality attributes like color, shrinkage ratio and rehydration capacity. Therefore, the RFVD + HAD method is recommended as a time and energy efficient drying technology for kiwifruits with a better moisture distribution and product quality.

1. Introduction

Approximately 4 million metric tons (Mt) of kiwifruits were produced worldwide in 2017, and about 50% of it originated from China (FAOSTAT, 2019). Microbial activity is a major cause of postharvest spoilage of fresh kiwifruits, which deteriorates its quality and shelf life (Zhou et al., 2018; Zhou, Li, Lyng, & Wang, 2018). Drying is one of the oldest preservation methods which rely on lowering the water activity of food products for improving their storage stability (Zhang et al., 2017). Recently, a great deal of attention has been paid to high-value foods, such as dehydrated fruits and soup mixes, due to their attractive appearances, desirable rehydration capacities and reduced packing/distribution costs (Zhang, Tang, Mujumdar, & Wang, 2006). However, there are some common problems associated with traditional drying of kiwifruits, such as hot air drying (HAD, Orikasa, Wu, Shiina, & Tagawa, 2008), vacuum drying (Fathi, Mohebbi, & Razavi, 2011) and osmotic dehydration (Castro-Giraldez, Fito, Dalla Rosa, & Fito, 2011), which include long drying times, low energy efficiency and poor product quality. There is, therefore, an increasing interest in developing alternative drying methods.

Radio frequency (RF) heating has been long proposed as an effective thermal treatment for various agricultural commodities for different purposes, such as disinfestation (Wang, Monzon, Johnson, Mitcham, & Tang, 2007; Zhou, Ling, Zheng, Zhang, & Wang, 2015; Zhou & Wang, 2016), pasteurization/sterilization (Li, Kou, Cheng, Zheng, & Wang, 2017; Liu et al., 2018; Xu et al., 2018), thawing (Palazoglu & Miran, 2017) and enzyme inactivation (Ling, Lyng, & Wang, 2018; Ling, Ouyang, & Wang, 2019). Because RF energy is theoretically more feasible for drying bulk materials owing to its deep penetration power and "moisture leveling" effect, RF heating has also been explored as a novel drying method for fresh fruits/vegetables (Zhou & Wang, 2019). However, improving heating/drying uniformity is still the major challenge for the implementations for RF drying techniques for high-moisture food products. As compared to other short-time RF heating treatments, such as RF disinfestation (4.3 min) of rice weevil (Zhou et al., 2015) and RF pasteurization (1.5 min) for inactivation of *E. coli* in in-shell almonds (Li et al., 2017), much longer times are needed for RF drying, such as hot air-assisted RF drying for in-shell walnuts (138 min) (Zhou, Gao, Mitcham, & Wang, 2018) and RF-vacuum drying (RFVD) for kiwifruit slices (270 min). Further, uneven heating has been noted and become critical, contributing to non-uniform drying patterns and quality variations. For example, the edge or corner over-heating has been reported during RF drying for in-shell macadamia nuts (Wang et al., 2014) and walnuts (Zhou, Gao, et al., 2018). Also, non-uniform

* Corresponding author at: College of Mechanical and Electronic Engineering, Northwest A&F University, Yangling, Shaanxi 712100, China.
E-mail address: shaojinwang@nwsuaf.edu.cn (S. Wang).

https://doi.org/10.1016/j.ifset.2019.102182
Received 23 February 2019; Received in revised form 12 June 2019; Accepted 20 June 2019
Available online 21 June 2019
1466-8564/

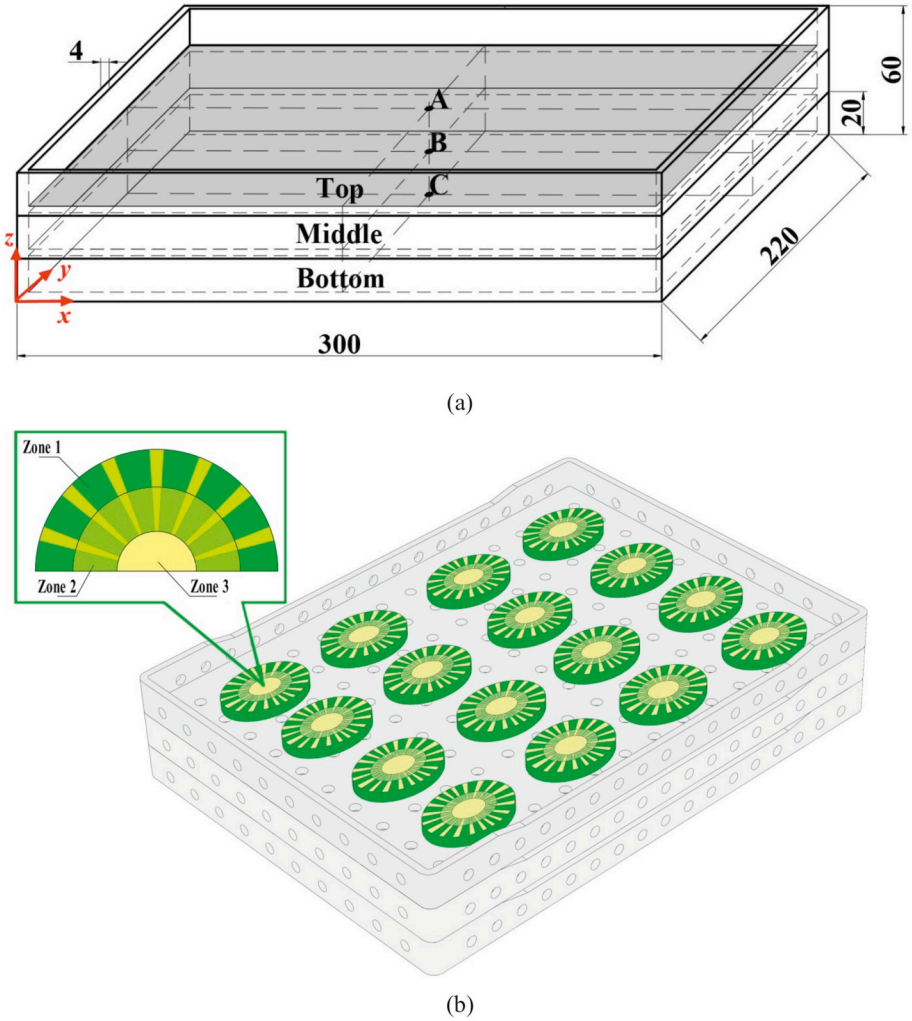

Fig. 1. Three-layer plastic container with three locations (A–C) for kiwifruit temperature measurements (all dimensions in mm) (a) and 3-D scheme of the container with three zones of the sample for moisture content measurements (b).

moisture distribution both within and among RFVD treated kiwifruit samples were observed in our recent study (Zhou, Xu, et al., 2018). Higher residual moisture levels were associated with the pericarp than in the center for RFVD dehydrated kiwifruit slices, whereas the residual moisture content of HAD treated ones became progressively higher from the periphery to the core. Thus, it was hypothesized that the tandem combination of volumetric dielectric heating (RF heating) and surface drying (hot air drying) might provide a drying protocol for improvement of drying uniformity, efficiency and product quality.

Determination of an appropriate sequence or combination operation is an important consideration for developing an effective RF combined drying process. RF heating can be used either before or after conventional drying (Zhou & Wang, 2019). For example, post-baking RF drying is a successful and commercially used process for the finish drying stage for cookies, with improvement in production efficiency and reduction of surface browning (Palazoglu, Coskun, Kocadagli, & Gokmen, 2012). However, some quality issues in final product, such as shell-cracks in nuts (Zhou, Gao, et al., 2018) and increase in fissure ratio or broken rate in milled rice (Jiao et al., 2017), could occur, making it less appealing to the consumer and reduce the marketability. Our recent studies also show that applying RFVD for HAD pre-dried fruits caused potential technical problems, including electric breakdown (arcing) and glow discharges. This was considered to be due to the concentration and redirection of RF electric fields on the irregular surfaces of the sample which are caused by severe shrinkage and case hardening developed during HAD, and edge effects of the surface in contact with the bottom electrodes, which in turn lead to “thermal runaway” phenomenon and sample scorching (Ramaswamy & Tang, 2008; Zhou & Wang, 2019; Zhou, Xu, et al., 2018). In the final stage of RFVD, localized sample temperature may increase far above the water boiling temperature and lead to product burning as it absorbs more and more RF energy. Also, owing to the large reduction of dielectric loss factor with moisture content (decreasing below 40–50% on a wet basis), the ability of dielectric materials to transform RF energy into thermal energy dramatically decreases (Zhou, Li, et al., 2018). RF heating is contributed both by dipole rotation and ionic conduction (Ramaswamy & Tang, 2008). With decreasing moisture content, the ionic conduction would play a larger role in the final stage of RF drying. By contrast, applying RFVD at the beginning could quickly raise sample temperature to moisture evaporation point and generate considerably high vapor pressure to transport moisture toward surface, and facilitate rapid hot air drying if used subsequently. Hence the combined RFVD and HAD would offer potential to improve drying uniformity, energy efficiency and final kiwifruit quality.

The objectives of this study were therefore (1) to study the heating characteristics of kiwifruit slices during HAD, RFVD, and combination of RFVD and HAD (RFVD + HAD), (2) to compare the drying uniformity of kiwifruit samples dried by the three methods, and (3) to calculate the drying energy efficiency, and evaluate the quality of final kiwifruit products.

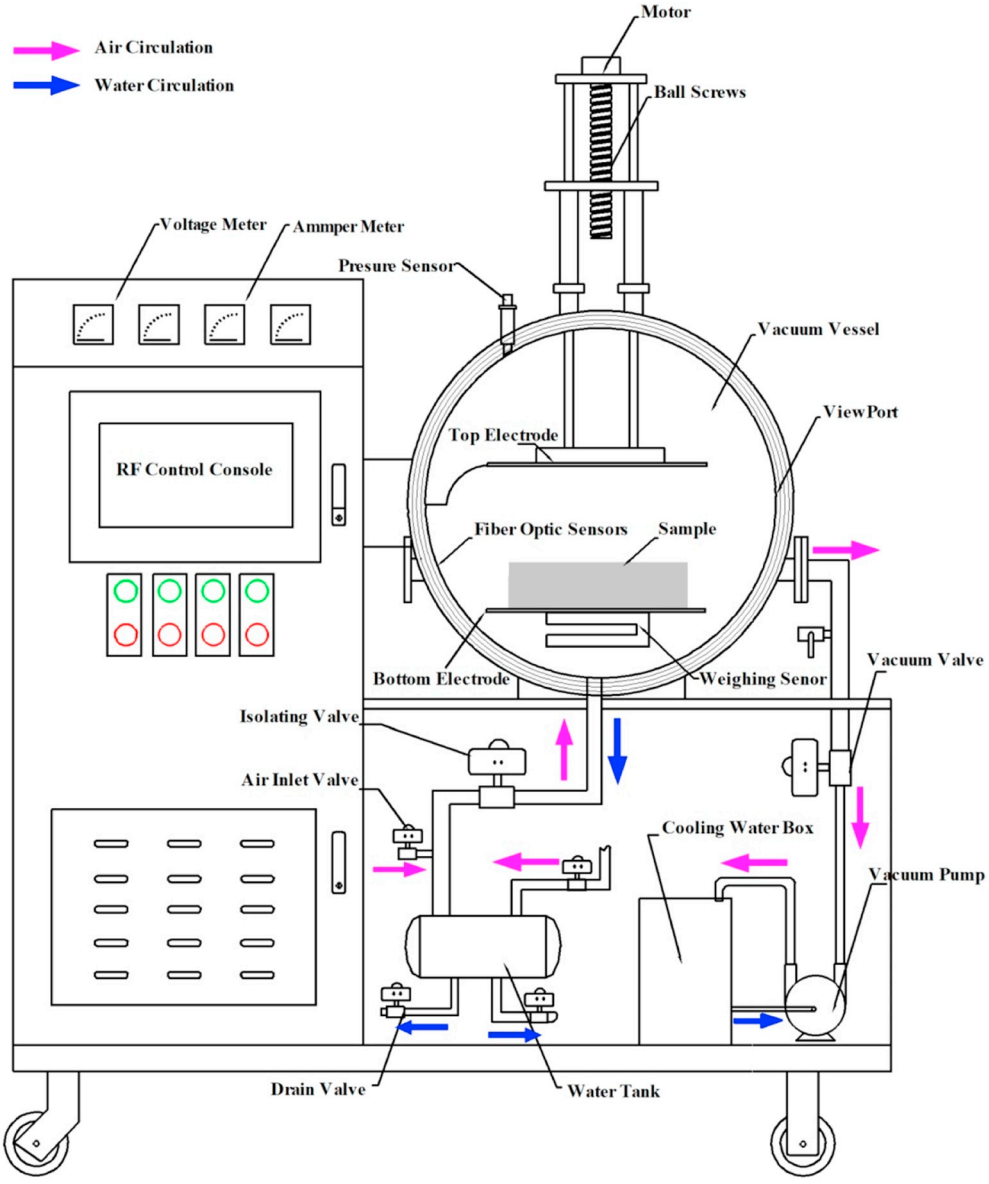

Fig. 2. Schematic view of 3 kW, 27.12 MHz RF-vacuum system showing plate electrodes, control system, and vacuum system. (Adapted from Zhou, Xu, et al. (2018)).

2. Material and methods

2.1. Material and sample preparation

Kiwifruits (*Actinidia deliciosa* cultivar "Hayward") were harvested from a local orchard in Zhouzhi, Shaanxi, China with the initial moisture content of 5.25 kg/kg on a dry basis (d.b.) in mid-October 2018. After careful visual check, fruits with similar size (length: 72.5 ± 1.4 mm, width: 59.3 ± 4.2 mm, weight: 128.3 ± 8.4 g) were immediately stored in a refrigerator (BC/BD-203HCZ, Haier Refrigeration Division, Qingdao, China) at 4 ± 1 °C and 90 ± 5% relative humidity (RH). Before each drying experiment, kiwifruits were equilibrated in an incubator (GD/JS4010, Haixiang Instrument & Equipment Co., Ltd., Shanghai, China) at 20 ± 0.5 °C and 30% RH overnight. The kiwifruits were then mechanically sliced and hand peeled into slices with thickness of 6.0 ± 0.3 mm and average diameter of 56.3 ± 2.4 mm. Thirty-six freshly prepared kiwifruit slices (523.1 ± 26.1 g) were placed in an orderly pattern on three polypropylene (PP) containers (300 mm *L* × 220 mm *W* × 20 mm *H*) with perforated screens on bottom and side walls, and each single-layer PP container was stacked on the top of each other to constitute a 3-tray drying set up with a top, middle and bottom tray (Fig. 1). Kiwifruit samples were segregated to avoid thermal damage at points of contact between samples during RF drying (Fig. 1(b)).

2.2. Drying procedures

2.2.1. RF-vacuum drying

Radio frequency-vacuum drying of kiwifruit slices was carried out in a 3 kW, 27.12 MHz RF-vacuum drying system (GJ-3-27-JY, Huasjiyuan High Frequency Equipment, Langfang, China) (Fig. 2). The detailed description of the RF-vacuum drying system can be found in Zhou, Xu, et al. (2018). The electrode gap could be varied between 20 and 300 mm by moving the top electrode plate (400 mm × 400 mm) to regulate RF energy for specific applications. The mass of test samples was measured continuously and recorded online by a weighting sensor (AT8106, Pengheng Electronic Inc., Shanghai, China) with a precision of 0.1 g mounted underneath the bottom electrode, and a four-channel fiber optic temperature sensor system (HQ-FTS-D120, Heqi Technologies Inc., Xian, China) with an accuracy of 0.5 °C was used for

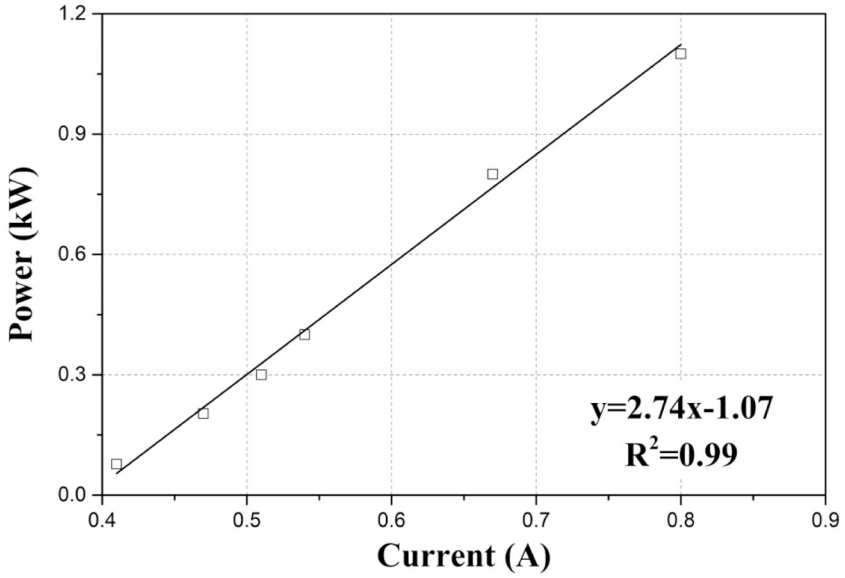

Fig. 3. Correlation between output power and electrical current of the RF-vacuum system using water loads.

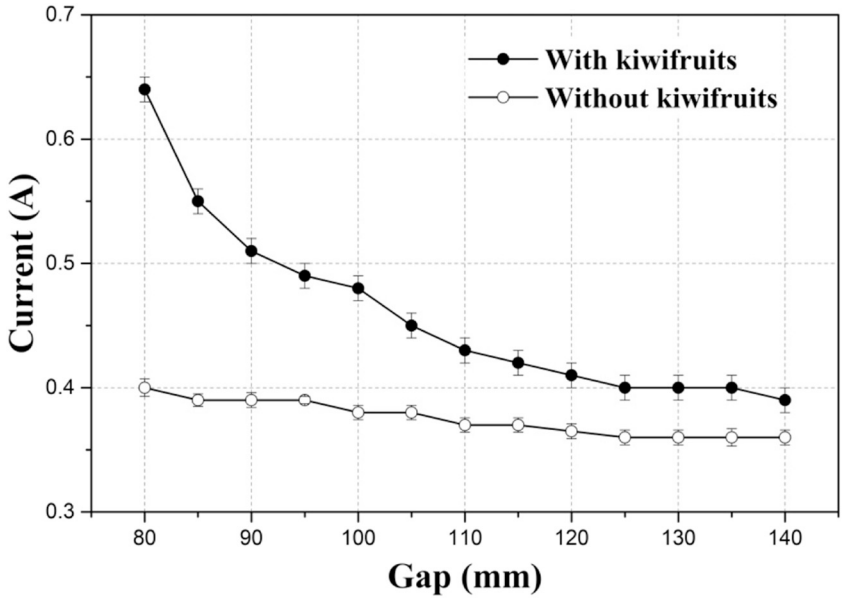

Fig. 4. Relationship between electrical current and RF electrode gap with or without kiwifruits in the three-layer container.

continuous temperature measurement. Based on our earlier studies (Zhou, Li, et al., 2018; Zhou, Xu, et al., 2018), the vacuum level for RFVD was set as 20.1 kPa to avoid arcing.

The RF-vacuum drying system could display the electric current used, but not RF power. The general relationship between RF output power and electric current was derived experimentally with a 500 g of pure water load according to the method of Zhou and Wang (2016). To select appropriate RF electrode gap, the three-tray container with kiwifruit samples was placed on the RF bottom electrode. After the vacuum reached 20.1 kPa and RF power was turned on, the electrical current (I, A) displayed on the control screen was recorded immediately as the electrode gap was adjusted from 80 to 140 mm with a distance interval of 5 mm. This test was repeated thrice. Electrode gaps of 85, 95 and 105 were preliminarily tested with four kiwifruit slices in the center of the middle plastic container and temperatures of their cores were measured by the four-channel fiber-optic sensors. The electrode gap was finally fixed according to the target average heating rate (2–3 °C/min) (Zhou & Wang, 2019) and standard deviation value during the first 10 min RFVD.

2.2.2. Hot air drying

Hot air drying of kiwifruit slices was carried out in a cross-flow tray drier (DHG-9030A, Precision & Scientific Instrument Co. Ltd., Shanghai, China) with an air flow rate of 2.0 m/s as measured by a rotary vane anemometer (LCA6000, AIRFLOW Instrumentation, Buckingham-215 Shire, UK) and RH ranging from 10 to 20% over the entire HAD process. The HAD temperature was set at 50 °C to reduce the discoloration and the loss of nutritional values of kiwifruits (Zhou, Xu, et al., 2018). The cabinet was preheated to 50 °C and maintained steady for 30 min before the three-tray PP container with fruits was placed on a wire mesh tray. During HAD, the kiwifruit samples were taken out of the hot air drier every 60 min; the sample mass was measured by an electronic balance (PTX-FA210, Huazhi Scientific Instrument, Co., Ltd., Fuzhou, China) with a precision of 0.01 g and the container was immediately returned to HAD for the continued drying.

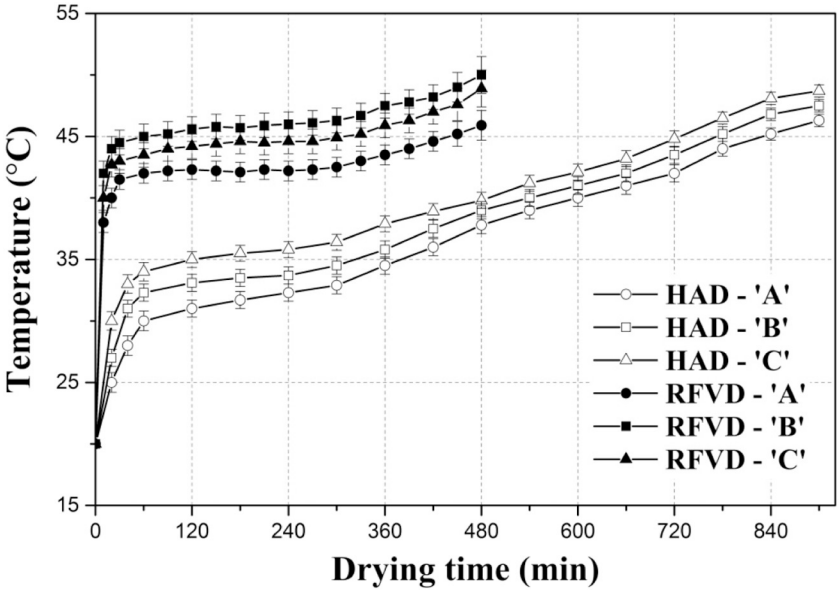

Fig. 5. Temperature-time histories of kiwifruit cores in the locations of A, B and C (Fig. 1(a)) when subjected to hot air drying (HAD) and radio frequency-vacuum drying (RFVD).

Table 1
Comparisons of the average surface temperature, heating uniformity index and moisture content (mean ± SD over 3 replicates) of the kiwifruit samples in the three-layer plastic container during the radio frequency-vacuum drying at seven average moisture contents (d.b.)

Average moisture content (d.b.)	5.00	4.00	3.00	2.00	1.00	0.50	0.25
Average surface temperature (°C)							
Top	34.1 ± 1.6	36.7 ± 1.4	36.8 ± 1.2	36.5 ± 0.7	36.6 ± 0.9	40.3 ± 2.6	50.3 ± 6.6
Middle	38.1 ± 1.6	40.9 ± 1.6	40.5 ± 1.4	40.3 ± 1.5	40.4 ± 1.4	43.2 ± 3.0	54.2 ± 7.5
Bottom	34.1 ± 1.7	40.2 ± 1.5	40.6 ± 1.4	39.1 ± 1.5	39.2 ± 1.3	42.5 ± 2.5	52.1 ± 7.0
Heating uniformity index (λ)							
Top	0.087 ± 0.003	0.064 ± 0.002	0.053 ± 0.001	0.045 ± 0.001	0.044 ± 0.001	0.121 ± 0.004	0.188 ± 0.005
Middle	0.068 ± 0.003	0.062 ± 0.003	0.056 ± 0.002	0.054 ± 0.003	0.055 ± 0.003	0.119 ± 0.005	0.192 ± 0.005
Bottom	0.089 ± 0.003	0.061 ± 0.002	0.056 ± 0.002	0.054 ± 0.003	0.055 ± 0.003	0.102 ± 0.004	0.190 ± 0.005
Moisture content (d.b.)							
Top	4.89 ± 0.05	3.84 ± 0.05	2.74 ± 0.04	1.72 ± 0.05	0.80 ± 0.03	0.28 ± 0.04	0.16 ± 0.03
Middle	5.02 ± 0.04	4.06 ± 0.04	3.06 ± 0.04	2.02 ± 0.03	1.05 ± 0.04	0.56 ± 0.04	0.27 ± 0.04
Bottom	5.08 ± 0.05	4.17 ± 0.04	3.18 ± 0.05	2.22 ± 0.04	1.26 ± 0.04	0.67 ± 0.05	0.33 ± 0.05

2.2.3. RF-vacuum drying in combination with hot air drying

The kiwifruit slices were dried by the RFVD until the average moisture content of kiwifruit samples decreased to 1.0 kg/kg (d.b.), and then transferred to the same HAD set up described earlier. The transition moisture content (1.0 kg/kg (d.b.)) was selected based on the RF-vacuum heating uniformity, which is explained in the following section. Once the RFVD process was completed, the RF unit power was turned off, and the three-tray PP container was transferred immediately to the HAD. The transfer time was <1 min and the sample temperature drop during the transfer process was <5 °C. In an industrial-scale RF drying, a moving conveyor could do such transfers on a continuous basis. To study the change in moisture content during the combined drying process, the sample mass was recorded every 5 s using the online system included in the RF-vacuum cavity during the RFVD, and then was measured every 60 min manually by taking out the sample container during the HAD.

All drying processes were continued until the moisture content of fruit samples decreased to 0.25 kg/kg (d.b.), with the corresponding water activity of approximately 0.60 (considerably lower than the 0.75 considered to be the upper limit for microbial stability). The target residual moisture content (0.25 kg/kg d.b.) of samples was achieved based on the initial moisture content and the transient mass loss during the drying processes, and final verification of moisture content in the dried product. Drying experiments were carried out in triplicates.

2.3. Surface and core temperature measurements

Owing to the interference between the fiber-optic sensor system and the thermal imaging camera system, two parallel tests (each in triplicate runs) were conducted under the same condition. For the first test, the kiwifruit slices in the central area on each tray (locations A, B and C at Fig. 1(a)) were used to determine the core temperature-time history by inserting fiber-optic sensor probes into slice cores during HAD and RFVD. In the parallel test, the plastic sample container was taken out and then top layer surface temperature of kiwifruit slices was mapped immediately using a thermal imaging camera (DM63, Zhejiang Dali Technology Co., Ltd., Hangzhou, China) with accuracy of ±2 °C. Middle and bottom layers were mapped sequentially and finally the trays were immediately returned to the RF cavity. Each thermal image took a very short time (<1 s) and the process was deemed not influence the drying profile. The thermal imaging camera was first calibrated against a type T thermocouple (TMQSS-020-6, Omega Engineering Ltd., CT, USA) with 0.8 s response time and an accuracy of ±0.2 °C. Based on the calibration, the emissivity of 0.95 was selected for the kiwifruit surface. The surface temperature profiles were used to estimate the RF heating uniformity.

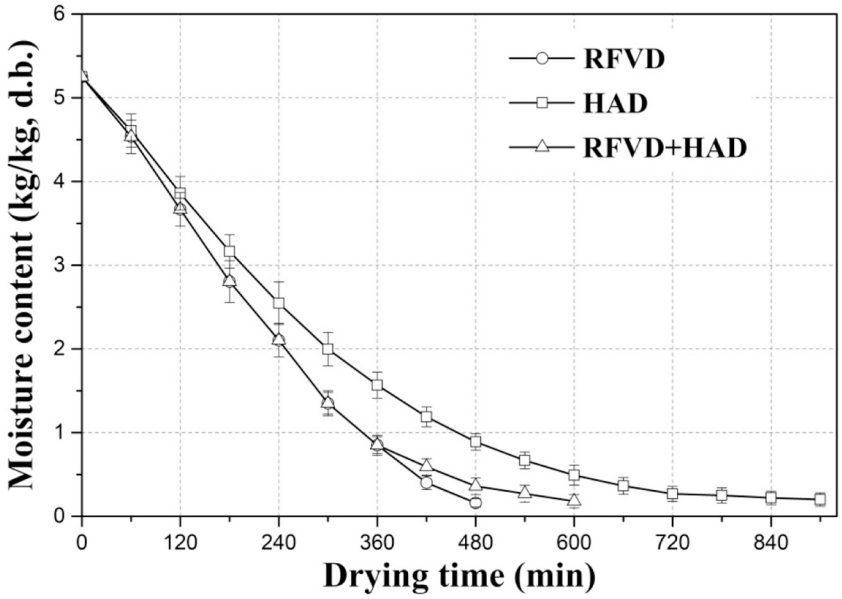

Fig. 6. Changes of moisture content of kiwifruits during the hot air drying (HAD), radio frequency-vacuum drying (RFVD) and combined RF-vacuum and hot air drying (RFVD + HAD).

2.4. Drying uniformity tests

Drying uniformity can be an important parameter for quantifying the quality impact performance of dielectric drying technologies and is closely associated with the change in the product quality during storage when the moisture gets redistributed (Zhang et al., 2017). In this study, drying uniformity tests involved quantification of both temperature and moisture distributions.

2.4.1. Heating uniformity and RFVD endpoint moisture content

A heating uniformity index (λ) was proposed in Wang et al. (2007) and always used to analyze RF heating uniformity:

$$\lambda = \frac{\Delta\sigma}{\Delta\mu} \tag{1}$$

where Δσ is the rise in standard deviation of material temperature (°C) and Δμ is the rise in mean temperatures (°C) over the RF treatment time.

To determine the endpoint moisture content of RFVD for transferring to HAD, the λ was calculated and compared when the average moisture content of kiwifruit samples decreased to 5.00, 4.00, 3.00, 2.00, 1.00, 0.50 and 0.25 kg/kg (d.b.) using the RFVD. The surface temperature distributions of top, middle and bottom trays were mapped by the infrared camera, and 45,000 individual temperature data in each thermal image were used for the calculation of λ. The heating uniformity test was repeated thrice.

2.4.2. Moisture distribution uniformity

To comprehensively characterize the drying uniformity of different drying methods, it is necessary to evaluate the moisture distribution not only within the individual dried kiwifruit but also among the samples (Zhou, Xu, et al., 2018).

For the moisture distribution among the dried kiwifruit samples, the moisture contents of dried samples in the middle sections were measured using the AOAC Official vacuum oven Method 925.40 (AOAC, 2005). For the moisture distribution within individual samples, kiwifruit slices were cut into three zones (i.e. outer pericarp, inner pericarp and core) (Fig. 1(b)) and moisture contents of each zone were measured by the vacuum oven method (AOAC, 2005). More detailed information about different zones of the kiwifruit slice can be found in Zhou, Xu, et al. (2018). These tests were repeated thrice, and the moisture contents were used to estimate the moisture distribution uniformity.

2.5. Energy efficiency

The average energy efficiency for RFVD (η_1, %) or HAD (η_2, %) was determined as a ratio of the total energy (P_{output}, W) absorbed by the kiwifruits to the power input (P_{input}, W) (Wang et al., 2007; Zhou & Wang, 2016):

$$\eta_1 = \frac{P_{output}}{P_{input}} \times 100\% = \frac{P_{output}}{P_{RFVD}} \times 100\% = \frac{mC_p(\Delta T/\Delta t) + m_w\lambda_1/\Delta t}{P(I)} \times 100\% \tag{2}$$

$$\eta_2 = \frac{P_{output}}{P_{input}} \times 100\% = \frac{P_{output}}{P_{HAD}} \times 100\% = \frac{mC_p(\Delta T/\Delta t) + m_w\lambda_2/\Delta t}{Ah(T_a - \overline{T_s})} \times 100\% \tag{3}$$

where P_{RFVD} and P_{HAD} are RF-vacuum and hot air system input power (W), respectively, m (kg) is the mass of kiwifruits in the three-layer container, C_p (J/kg °C) is the average specific heat of kiwifruits (3160 J/kg °C) determined by a differential scanning calorimeter (Q2000, TA Instruments, New Castle, PA, USA), ΔT (°C) is the average temperature increase in fruit samples, Δt (s) is the drying time, m_w (kg) is the mass of vaporized water, λ_1 and λ_2 are the latent heat (J/kg) under vacuum (20.1 kPa) and normal pressure (101.3 kPa), A (m^2) is the total surface area (0.1279 m^2) of thirty-six kiwifruit slices exposed to air, and equals to the top surface area (0.0897 m^2) plus cylindrical area (0.0382 m^2) of the fruit slices, h (W/m^2 °C) is the convective heat transfer coefficient and was estimated to be 85 W/m^2 °C for forced convection (Ozisik, 1985), T_a (°C) is the temperature of hot air, and $\overline{T_s}$ (°C) is average surface temperature of samples during drying. Heat loss and moisture evaporation were assumed to be negligible when samples were transferred from RFVD to the HAD.

2.6. Quality evaluation

The quality attributes including color, rehydration capacity (*RC*) and shrinkage ratio (*SR*), and water activity (a_w) were evaluated before and after different drying treatments. The a_w was measured using a water activity meter (Model 4TE, Decagon Devices, Inc., Pullman, WA, USA). The color parameters (L^*, a^*, b^* and ΔE) were measured and calculated by a computer vision system (Zhou, Xu, et al., 2018). The *RC* was calculated as a percentage of mass gain from the initial one and

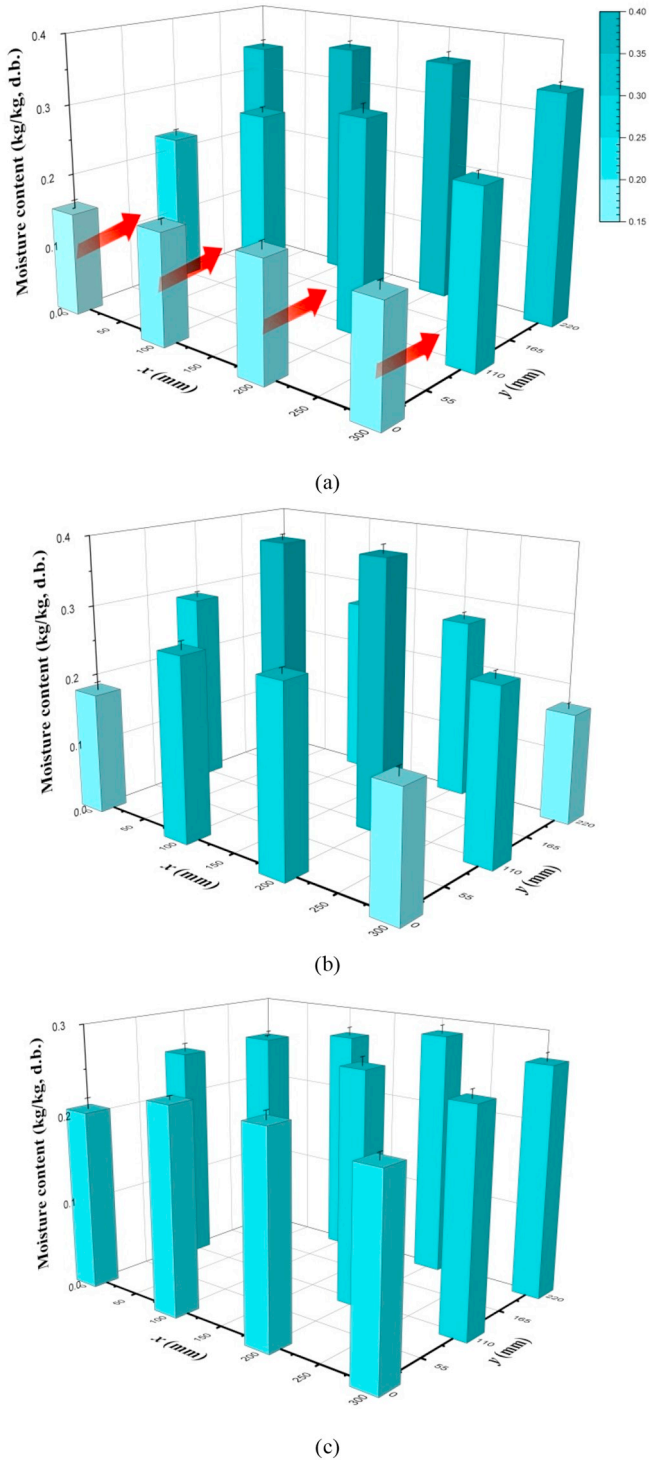

Fig. 7. Moisture content of hot air (a), RF-vacuum (b) and combined RF-vacuum and hot air (c) dried kiwifruit samples in the middle layer with y-axis (Fig. 1a) parallel to the hot air flow.

determined by immersing dehydrated kiwifruit samples into the hot water (50 °C) for 15 min (Zhou, Xu, et al., 2018). The *SR* was measured by a toluene displacement method and expressed by the following equation:

$$\mathrm{SR} = \frac{V_0 - V}{V_0} \times 100\% \quad (4)$$

where *SR* is the percentage of shrinkage (dimensionless), V_0 and V are the sample volume values (m^3) before and after drying, respectively.

2.7. Statistical analysis

All numerical results were expressed as mean and standard deviations (SDs) of triplicate runs. Significant differences test was performed using the Microsoft Excel variance procedure (Microsoft Office Excel, 2010) to determine difference between the means ($P < 0.05$).

3. Results and discussion

3.1. RF electrode gap determination

Fig. 3 shows the correlation between output power and electrical current of the RF-vacuum drying system using water loads within an electrode gap range of 80 to 140 mm. The linear model ($P = 2.74x$-1.07) provided the best fit for power calibration curve with R^2 of 0.99 and thus assumed adequate to be used for output power estimation of the RF-vacuum drying system. The relationship between electrical current and electrode gap under the vacuum of 20.1 kPa for the three-tray plastic container with or without kiwifruit slices is shown in Fig. 4. The electrical current decreased with increasing electrode gap, with a more pronounced decrease at smaller gaps (80 to 125 mm), and thereafter remained relatively stable. But without kiwifruit samples, the electrical value was almost a constant with a narrow fluctuation between 0.36 and 0.40 A as the electrode gap decreased. The RFVD heating rates of samples during the first 10 min at the center of the middle layer were 5.59 ± 1.36 °C/min, 2.90 ± 0.48 °C/min and 1.56 ± 0.42 °C/min under electrode gaps of 85 mm, 95 mm and 105 mm, respectively. The heating rate decreased with increasing electrode gap due to the decline of RF electric field intensity (Huang, Zhu, Yan, & Wang, 2015). To obtain the previously targeted heating rate (2–3 °C/min) and acceptable heating uniformity, the electrode gap of 95 mm was finally selected for the further RFVD experiments.

3.2. Core temperature-time histories

Fig. 5 shows temperature profiles of kiwifruit cores in three locations (A, B and C) of the plastic sample container (Fig. 1) during HAD and RFVD. It took approximately 30 and 660 min to raise sample core temperatures from 20 °C to 40 °C for RFVD and HAD, respectively, indicating that RFVD would provide the desired rapid heating rates which HAD failed to deliver. The advantages of rapid RF heating over hot air heating have also been observed in earlier studies (Zhou et al., 2015; Zhou, Gao, et al., 2018). In the final drying stage, the kiwifruit sample temperatures in both RFVD and HAD continued to increase. Additionally, the highest temperature during RFVD was found in the location B, followed by C and A, because of the higher RF electric filed distribution in the middle layer than the other layers (Huang et al., 2015). By contrast, the core temperature was lower at the location B than at A and C during the HAD process, mainly because of the higher heat and moisture loss in the top and bottom layers.

3.3. Heating uniformity and conversion moisture content

Table 1 shows a detailed comparison of the average surface temperature, RF heating uniformity index (λ) and vertical moisture distribution profile for kiwifruit slices in the three-tray set up during RFVD. The highest average surface temperature was found on the middle tray over the entire RFVD, probably because the other two trays were exposed to either air on the top or electrode plate in the bottom. The surface temperature at top was a little lower than that of the bottom layer due to more heat loss from the top caused by higher evaporation rates, which also corresponded to the vertical profile of moisture content distribution (Table 1). The surface temperature in each tray remained almost constant with decreasing moisture content until 1.00 kg/kg (d.b.), but it considerably increased in the final stage of the RFVD process. The likely explanation for the dramatic temperature

Table 2
Moisture content (means ± SD over three replicates, d.b.) of three tissue zones (Fig. 1b) of kiwifruit slices before and after three drying treatments.

Treatments	Fresh	HAD	RFVD	RFVD + HAD
Whole sample	5.25 ± 0.31aA*	0.26 ± 0.04bB	0.24 ± 0.03bB	0.25 ± 0.03aB
Zone 1	5.67 ± 0.46aA	0.14 ± 0.03cD	0.29 ± 0.02aB	0.22 ± 0.03aC
Zone 2	4.98 ± 0.44aA	0.23 ± 0.03bB	0.24 ± 0.02bB	0.26 ± 0.03aB
Zone 3	4.53 ± 0.42bA	0.41 ± 0.04aA	0.18 ± 0.03cC	0.28 ± 0.04aB

HAD: hot air drying; RFVD: radio frequency-vacuum drying; RFVD + HAD: combined radio frequency-vacuum and hot air drying.
* Different lower and upper case letters indicate that means are significantly different at $P = 0.05$ among zones and drying treatments, respectively;

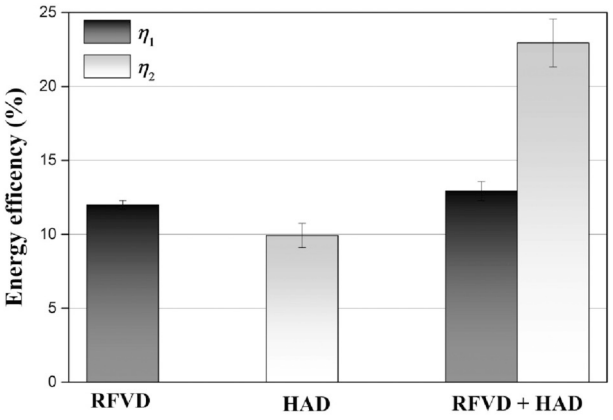

Fig. 8. The energy efficiency of the RF-vacuum and hot air system estimated for drying kiwifruit slices.

rise is that the absorbed RF energy was larger than that required for evaporation since smaller quantities of moisture is available in the finish drying stage (Zhang et al., 2006). As a result, the "dry" sample temperatures even rose above the boiling water temperature (60 °C, at the vacuum level). At the beginning of RFVD drying, the λ values gradually decreased and then remained relatively stable at between 0.044 and 0.055 until the sample moisture content was reduced to 1.00 kg/kg (d.b.), suggesting that the use of vacuum could improve the RF heating uniformity by limiting the sample maximum temperature (Zhou, Li, et al., 2018; Zhou, Xu, et al., 2018). As RFVD progressed, however, both λ values and the vertical moisture content variation substantially increased. The reduction of RFVD heating uniformity also resulted in the clear increase in standard deviation (SD) values of horizontal profile of temperature distributions during the final RFVD process. These results indicated that to obtain acceptable RFVD heating uniformity and vertical moisture profile balancing, it is better to apply RFVD up to the average moisture content of kiwifruit samples decreasing to 1.00 kg/kg (d.b.). Therefore, the target moisture content for transferring the samples from RFVD to HAD was set at 1.00 kg/kg (d.b.) for RFVD + HAD process.

3.4. Drying characteristics

Fig. 6 shows that it required 480, 600 and 900 min to reduce the initial sample moisture content (5.25 kg/kg, d.b.) to target level (0.25 kg/kg, d.b.) for RFVD, RFVD + HAD and HAD, respectively. It was noted that approximately 50% reduction in drying time was achieved using RFVD as compared to HAD and about 35% when RFVD + HAD vs. HAD. The RFVD would be the best choice from the point of view of the drying time; however, it needs to be considered in relation to the product quality as well. The combination of RF heating and vacuum drying is effective, because one has the capacity to add energy and push the water out of the fruit while the other can pull it out of the system. The moisture content continuously decreased with RFVD drying time, but slowed at the final drying process possibly due to limited mass transfer from inside the fruit (Wang et al., 2014). It took 720 min for HAD to reduce fruit moisture content to around 0.25 kg/kg (d.b.), after which the drying rate considerably dropped largely due to the severe surface shrinkage and case hardening effects (Zhang et al., 2017). For the RFVD + HAD, kiwifruit samples were dried to 1.00 kg/kg (d.b.) with 360 min of RFVD, plus 240 min of HAD to result in the target moisture content of 0.25 kg/kg (d.b.). This may be because the RFVD generated heat within materials due to molecular friction as a result of dipolar relaxation and ionic conduction (Zhou, Xu, et al., 2018), leading to high heating and drying rates in the initial drying process, and the moisture was pushed out from the interior to the surface by generated vapor pressure, making it easier and shorter for the HAD to remove this surface water in the finish drying stage.

3.5. Moisture distribution uniformity

3.5.1. Moisture distribution among samples

Fig. 7 shows the moisture distribution of dried kiwifruit slices over 12 locations in the middle layer obtained after three drying methods. The moisture reduction of HAD samples were in line with the direction of the hot air and the moisture removal potential diminished as the air moved forward. Fresh and dry air hit the front of the tray and as they took the moisture from the sample, its relative humidity increased and velocity decreased, and both of which are attributed to reducing the drying rates (Zhou, Xu, et al., 2018). The moisture contents of RFVD samples were much lower around the edges and corners than those at the center, due to the higher electric field strength (Huang et al., 2015). However, the transient moisture variations in RFVD + HAD samples were much more uniform due to the avoidance of RF runaway heating and the time reduction of hot air finish drying, demonstrating the advantage for using the combination RFVD + HAD process as opposed to using either of them individually. This can override the disadvantage of the somewhat higher drying time associated with RFVD + HAD over RFVD.

Table 3
Quality characteristics (means ± SD over three replicates) of kiwifruit samples before and after three drying treatments.

	L^*	a^*	b^*	ΔE	Water activity (a_w)	Shrinkage (%)	Rehydration capacity (%)
Fresh	41.2 ± 1.5a#	−9.0 ± 0.1d	26.1 ± 0.5a	–	0.99 ± 0.00a	–	–
HAD	28.9 ± 1.6d	−0.1 ± 0.1a	18.8 ± 0.7c	16.9 ± 3.2a	0.58 ± 0.04b	76.1 ± 4.3b	89.6 ± 1.8c
RFVD	33.7 ± 1.2c	−3.4 ± 0.3b	19.3 ± 0. 6b	11.6 ± 2.3b	0.59 ± 0.04b	59.4 ± 5.5a	108.0 ± 1.6a
RFVD + HAD	38.4 ± 1.1b	−4.8 ± 0.3c	25.1 ± 0.7a	5.2 ± 2.0c	0.58 ± 0.03b	64.6 ± 3.4a	96.4 ± 1.6b

HAD: hot air drying; RFVD: radio frequency-vacuum drying; RFVD + HAD: combined radio frequency-vacuum and hot air drying.
Different lower case letter indicates that means are significantly different at P = 0.05 among drying methods;

3.5.2. Moisture distribution within individual samples

Table 2 shows the moisture contents in the three designated zones within the kiwifruit slice before and after drying by different methods. With RFVD, higher moisture content was associated with the core than at periphery while the moisture content decreased progressively from the center to the pericarp with the HAD process. This was because thermal energy was generated within fruit slices using RF energy, whereas the HAD depends on surface heating by convection and internal heating by conduction (Zhou & Wang, 2019). By contrast, no significant difference ($P > 0.05$) was found in moisture contents in the three zones for kiwifruit samples subjected to the RFVD + HAD method. The RFVD raised sample temperatures inside and moved the moisture to the surface and the HAD removed the outside moisture. Therefore, the combination of surface heating of the HAD and internal heating of RFVD resulted in more uniform moisture distributions within fruit samples as compared to single drying technologies. Since the heating mechanisms of microwave (MW) and RF waves are the same, except that the RF may have a deeper penetration power (Zhou & Wang, 2019), the similar effect of combined drying methods on moisture distribution within individual samples has also been reported in combined MW and air drying (Pu & Sun, 2016, 2017).

3.6. Energy efficiency

Fig. 8 compares the energy efficiency of RFVD, HAD and RFVD + HAD systems. Based on Eqs. (2) and (3), energy efficiency (η_1) for RFVD + HAD (12.93%) was slightly higher than that of the RFVD (11.98%), whereas the η_2 was significantly higher in the combined drying (22.93%) than that in the HAD (9.92%). There are several reasons for the considerable increase in η_2. Firstly, moisture within samples absorbed RF energy and was pushed from the interior to the surface by generated vapor pressure (Zhou, Xu, et al., 2018), so it was easier for the HAD to remove this surface water in the finish drying stage. Also, RFVD heating could reduce the surface shrinkage (swelling effect) and generate porous structure (puffing effect) (Zhang et al., 2006), which might facilitate better moisture migration during subsequent HAD. Finally, it was assumed that there existed some bound water dispersion during the RF heating (Zhou, Li, et al., 2018), which might make HAD more efficient to remove during the final drying stage. Low-field nuclear magnetic resonance method could be used to verify the hypothesis. In general, applying HAD after RFVD could improve the energy efficiency (η_1 and η_2) and might be more efficient as a combined drying method than the single drying method in practical applications.

3.7. Quality evaluation

Table 3 shows the quality of kiwifruits before and after drying by the three methods. The associated highest L^* and b^* value as well as lowest a^* value were with RFVD + HAD dried kiwifruit products, suggesting that the combined drying method produced brighter and greener samples. Also, the total color change (ΔE) for RFVD + HAD was significantly lower than the other drying methods ($P < 0.05$). However, the combination drying process still showed color deterioration because of chlorophyll degradation and possible Maillard reaction (due to heat). Therefore, further study is necessary to develop some effective pretreatments, such as blanching or using of antioxidants, to improve the color of final kiwifruit products and prevent enzymatic browning during storage. The average water activity (a_w) of all dried kiwifruit slices were below 0.60 and much lower than 0.75 which is generally recognized as the minimum required for microbial growth and activity. Although dried samples exhibited shrinkage trend during drying due to the compressive stress and shrinkage of cells (Jiang, Zhang, Fang, Mujumdar, & Xu, 2016), the *SR* values of RFVD and RFVD + HAD processed kiwifruit samples were significantly lower ($P < 0.05$) than those of HAD treated samples. RF drying could reduce the surface shrinkage (swelling effect due to rapid outward effusion of moisture) and generate loose and porous structure (puffing effect) (Ling et al., 2018; Zhang et al., 2006), and thereby test samples could maintain a regular shape. This enhanced porosity created in samples could also give rise to higher water absorption capacity (Zhou, Xu, et al., 2018), so the rehydration capacities of both RFVD and RFVD + HAD samples were significantly higher than those of HAD samples ($P < 0.05$). In some earlier studies, high water absorption capacity has also been observed in MW-vacuum dried fruits, such as blueberries (Zielinska & Michalska, 2016) and carrots (Zhang et al., 2006).

4. Conclusions

When vacuum (20.1 kPa) was applied, an electrode gap of 95 mm was found suitable for RFVD protocol based on desirable heating rate and temperature variation. The RFVD heating uniformity index remained at acceptable levels until the moisture content decreased to 1.00 kg/kg which was thereby selected as the target moisture for switching the drying process from RFVD to HAD. Individual drying methods (RFVD and HAD) showed considerable non-uniform drying patterns, whereas the RFVD + HAD not only resulted in a more uniform moisture distribution within the individual samples, but also lowered sample to sample variations. The average energy efficiencies were improved from 11.98% to 12.93% and from 9.92% to 22.93% for RF-vacuum system and hot air system, respectively, by using RFVD + HAD. In addition, the combined drying method ensured better final kiwifruit product quality in terms of color, rehydration capacity and shrinkage ratio. Therefore, the RFVD + HAD treatment protocol could provide a more uniform, efficient and practical drying method for kiwifruits with higher quality attributes.

Declaration of Competing Interest

The authors declare that they have no known competing financial interests or personal relationships that could have appeared to influence the work reported in this paper.

Acknowledgements

This research was conducted in the College of Mechanical and Electronic Engineering, Northwest A&F University, and supported by research grants from National Key Research and Development Program of China (2017YFD0400900, 2016YFD0401000), Key Research and Development Program in Shaanxi Province of China (Project No. 2018NY-105) and Key Laboratory of Post-Harvest handling of fruits, Ministry of Agriculture (GPCH201703). The authors also appreciate Shuming Zhang in Nankai University for her technical assistance during the experiments.

References

AOAC (2005). *Official methods of analysis* (16th ed.). Washington, DC: Association of Official Analytical Chemists.

Castro-Giraldez, M., Fito, P. J., Dalla Rosa, M., & Fito, P. (2011). Application of microwaves dielectric spectroscopy for controlling osmotic dehydration of kiwifruit (*Actinidia deliciosa* cv Hayward). *Innovative Food Science & Emerging Technologies, 12*(4), 623–627.

FAOSTAT (2019). Food and Agriculture Organization of the United States. http://www.fao.org/faostat/en/#data, Accessed date: January 2019.

Fathi, M., Mohebbi, M., & Razavi, S. M. A. (2011). Effect of osmotic dehydration and air drying on physicochemical properties of dried kiwifruit and modeling of dehydration process using neural network and genetic algorithm. *Food and Bioprocess Technology, 4*(8), 1519–1526.

Huang, Z., Zhu, H., Yan, R., & Wang, S. (2015). Simulation and prediction of radio frequency heating in dry soybeans. *Biosystems Engineering, 129*, 34–47.

Jiang, H., Zhang, M., Fang, Z. X., Mujumdar, A. S., & Xu, B. G. (2016). Effect of different dielectric drying methods on the physic-chemical properties of a starch-water model system. *Food Hydrocolloids, 52*, 192–200.

Jiao, S., Sun, W., Yang, T., Zou, Y., Zhu, X., & Zhao, Y. (2017). Investigation of the feasibility of radio frequency energy for controlling insects in milled rice. *Food and Bioprocess Technology, 10*(4), 781–788.

Li, R., Kou, X. X., Cheng, T., Zheng, A. J., & Wang, S. J. (2017). Verification of radio frequency pasteurization process for in-shell almonds. *Journal of Food Engineering, 192*, 103–110.
Ling, B., Lyng, J. G., & Wang, S. (2018). Radio-frequency treatment for stabilization of wheat germ: Dielectric properties and heating uniformity. *Innovative Food Science & Emerging Technologies, 48*, 66–74.
Ling, B., Ouyang, S., & Wang, S. (2019). Radio-frequency treatment for stabilization of wheat germ: Storage stability and physicochemical properties. *Innovative Food Sci. Emerg. Technol. 52*, 158–165.
Liu, S. X., Ozturk, S., Xu, J., Kong, F. B., Gray, P., Zhu, M. J., ... Tang, J. M. (2018). Microbial validation of radio frequency pasteurization of wheat flour by inoculated pack studies. *Journal of Food Engineering, 217*, 68–74.
Orikasa, T., Wu, L., Shiina, T., & Tagawa, A. (2008). Drying characteristics of kiwifruit during hot air drying. *Journal of Food Engineering, 85*(2), 303–308.
Ozisik, M. N. (1985). *Heat transfer: A basic approach.* New York: McGraw-Hill.
Palazoglu, T. K., Coskun, Y., Kocadagli, T., & Gokmen, V. (2012). Effect of radio frequency postdrying of partially baked cookies on acrylamide content, texture, and color of the final product. *Journal of Food Science, 77*(5), E113–E117.
Palazoglu, T. K., & Miran, W. (2017). Experimental comparison of microwave and radio frequency tempering of frozen block of shrimp. *Innovative Food Science & Emerging Technologies, 41*, 292–300.
Pu, Y. Y., & Sun, D. W. (2016). Prediction of moisture content uniformity of microwave-vacuum dried mangoes as affected by different shapes using NIR hyperspectral imaging. *Innovative Food Science & Emerging Technologies, 33*, 348–356.
Pu, Y. Y., & Sun, D. W. (2017). Combined hot-air and microwave-vacuum drying for improving drying uniformity of mango slices based on hyperspectral imaging visualisation of moisture content distribution. *Biosystems Engineering, 156*, 108–119.
Ramaswamy, H., & Tang, J. (2008). Microwave and radio frequency heating. *Food Science and Technology International, 14*(5), 423–427.
Wang, S., Monzon, A., Johnson, J. A., Mitcham, E. J., & Tang, J. (2007). Industrial-scale radio frequency treatments for insect control in walnuts I: Heating uniformity and energy efficiency. *Postharvest Biology and Technology, 45*(2), 240–246.
Wang, Y., Zhang, L., Johnson, J., Gao, M., Tang, J., Powers, J. R., & Wang, S. (2014). Developing hot air-assisted radio frequency drying for in-shell macadamia nuts. *Food and Bioprocess Technology, 7*(1), 278–288.
Xu, J., Liu, S., Tang, J., Ozturk, S., Kong, F., & Shah, D. H. (2018). Application of freeze-dried Enterococcus faecium NRRL B-2354 in radio-frequency pasteurization of wheat flour. *LWT- Food Science and Technology, 90*, 124–131.
Zhang, M., Chen, H. Z., Mujumdar, A. S., Tang, J. M., Miao, S., & Wang, Y. C. (2017). Recent developments in high-quality drying of vegetables, fruits, and aquatic products. *Critical Reviews in Food Science and Nutrition, 57*(6), 1239–1255.
Zhang, M., Tang, J., Mujumdar, A. S., & Wang, S. (2006). Trends in microwave-related drying of fruits and vegetables. *Trends in Food Science & Technology, 17*(10), 524–534.
Zhou, L. Y., Ling, B., Zheng, A. J., Zhang, B., & Wang, S. J. (2015). Developing radio frequency technology for postharvest insect control in milled rice. *Journal of Stored Products Research, 62*, 22–31.
Zhou, L. Y., & Wang, S. J. (2016). Industrial-scale radio frequency treatments to control *Sitophilus oryzae* in rough, brown, and milled rice. *Journal of Stored Products Research, 68*, 9–18.
Zhou, X., Gao, H., Mitcham, E. J., & Wang, S. (2018). Comparative analyses of three dehydration methods on drying characteristics and oil quality of in-shell walnuts. *Drying Technology, 36*(4), 477–490.
Zhou, X., Li, R., Lyng, J. G., & Wang, S. (2018). Dielectric properties of kiwifruit associated with a combined radio frequency vacuum and osmotic drying. *Journal of Food Engineering, 239*, 72–82.
Zhou, X., & Wang, S. (2019). Recent developments in radio frequency drying of food and agricultural products: A review. *Drying Technology, 37*(3), 271–286.
Zhou, X., Xu, R., Zhang, B., Pei, S., Liu, Q., Ramaswamy, H. S., & Wang, S. (2018). Radio frequency-vacuum drying of kiwifruits: Kinetics, uniformity, and product quality. *Food and Bioprocess Technology, 11*(11), 2094–2109.
Zielinska, M., & Michalska, A. (2016). Microwave-assisted drying of blueberry (*Vaccinium corymbosum* L.) fruits: Drying kinetics, polyphenols, anthocyanins, antioxidant capacity, colour and texture. *Food Chemistry, 212*, 671–680.